Room-temperature emission at telecom wavelengths from silicon photonic crystal nanocavities

R. Lo Savio,[1] S. L. Portalupi,[1] D. Gerace,[1] A. Shakoor,[2] T. F. Krauss,[2] L. O'Faolain,[2] L. C. Andreani,[1] and M. Galli[1,a)]
[1]*Dipartimento di Fisica "A. Volta," Università di Pavia, 27100 Pavia, Italy*
[2]*School of Physics and Astronomy, University of St. Andrews, Fife KY16 9SS, St. Andrews, United Kingdom*

(Received 2 March 2011; accepted 25 April 2011; published online 18 May 2011)

Strongly enhanced light emission at wavelengths between 1.3 and 1.6 μm is reported at room temperature in silicon photonic crystal (PhC) nanocavities with optimized out-coupling efficiency. Sharp peaks corresponding to the resonant modes of PhC nanocavities dominate the broad sub-bandgap emission from optically active defects in the crystalline Si membrane. We measure a 300-fold enhancement of the emission from the PhC nanocavity due to a combination of far-field enhancement and the Purcell effect. The cavity enhanced emission has a very weak temperature dependence, namely less than a factor of 2 reduction between 10 K and room temperature, which makes this approach suitable for the realization of efficient light sources as well as providing a quick and easy tool for the broadband optical characterization of silicon-on-insulator nanostructures.
 [doi:10.1063/1.3591174]

Light emission in crystalline silicon (c-Si) has been a subject of intense and thorough research over the past two decades.[1] In fact, although silicon is an indirect band gap semiconductor, the development of an all-silicon device showing efficient light emission at room temperature would entail enormous benefits. Many different strategies have been explored to make silicon an efficient infrared emitter at strategic telecom wavelengths, including doping with rare-earth atoms,[2,3] or exploiting optically active structural defects.[4–8]

Though very promising, devices based on silicon sub-band gap luminescence are still impractical because emission intensity is strongly quenched for temperatures above $\simeq$100 K and becomes almost undetectable at room temperature. In such devices, enhancement of light emission relies on the combination of two complementary strategies, defect engineering and device engineering. On the one hand, the former route aims to increasing the efficiency of active centers by reducing nonradiative recombination. On the other hand, field-confining photonic nanostructures such as high-Q photonic crystal (PhC) cavities can increase light emission through the Purcell effect and optimization of the light extraction efficiency. Enhanced light emission and low-threshold lasing has been extensively reported in III-V based[9] and in silicon-compatible devices.[10,11] However, their application to increasing light emission from c-Si has been limited to the narrow spectral region of indirect band-edge recombination at 1.1 μm wavelength.[12–14]

In this letter, we report the observation of enhanced room-temperature photoluminescence (PL) from silicon PhC nanocavities with resonant modes in the range 1.3–1.6 μm, well below the Si band gap. The broad sub-bandgap emission feeding the cavity modes is attributed to optically active defects introduced during the manufacturing process of the silicon-on-insulator (SOI) wafers.

Silicon PhC nanocavities consisting of three-missing holes in a triangular lattice of air-holes (L3) were fabricated by means of e-beam lithography and reactive ion etching on a SOI wafer (220 nm thick silicon on 2000 nm of silica-purchased from SOITEC). The fabrication procedure is the same as that reported in Ref. 15. Several L3 cavities with a lattice constant of a=420 nm and a hole radius of r/a =0.29 were fabricated. To increase the light emission in the vertical direction, far-field optimization was applied by modifying the diameter of the holes around the PhC cavities by a quantity Δr=+18 and −18 nm (see Ref. 15). Furthermore, optimization of the radius and position of the holes adjacent to the cavity was performed in order to obtain high Q factors.[16] A scanning electron microscope (SEM) image of a typical L3 PhC nanocavity is shown in inset of Fig. 1.

Confocal micro-PL (μPL) from the planar PhC nanocavities was measured at variable temperature in the 1.0–1.6 μm spectral range using a highly stable continuous-flow He cryostat (Janis ST500). The samples were excited with a Nd:YAG laser at λ=532 nm, which was focused to a spot of ~1 μm diameter at the center of the PhC nanocavi-

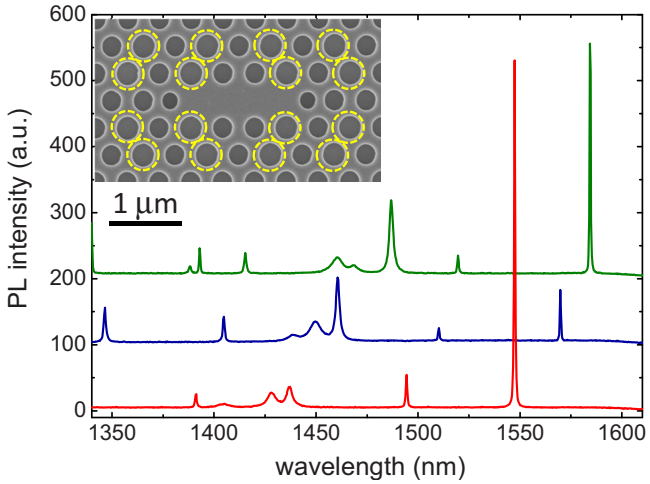

FIG. 1. (Color online) Room-temperature μPL spectra of modified L3 PhC nanocavities with Δr=−18 nm (top curve), 0 nm (middle curve), and +18 nm (bottom curve). Curves are shifted vertically for clarity. Inset shows a SEM image of the PhC nanocavity with Δr=+18 nm. Dashed circles indicate the modified holes.

a)Electronic mail: matteo.galli@unipv.it.

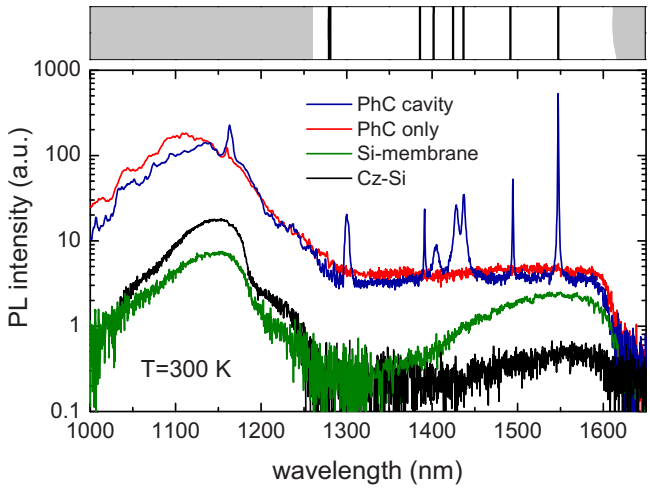

FIG. 2. (Color online) Broadband room-temperature μPL spectra of L3 nanocavity with Δr=+18 nm, reference PhC membrane, unpatterned Si membrane, and reference Cz-Si sample. Excitation power is 500 μW in all cases. The sharp drop at 1620 nm, common to all spectra, is due to the detector cutoff. The top panel shows the calculated spectrum, including cavity resonances and PhC band edges.

ties by means of a high numerical aperture (NA=0.8) microscope objective. Light emitted from the nanocavities was then collected through the same objective, filtered by a pinhole and sent to a grating spectrometer equipped with an InGaAs array detector. The use of high NA collection optics and careful alignment of the sample are essential for observing the very weak PL signals, as reported below.

Figure 1 shows the room-temperature μPL spectra collected for L3 PhC nanocavities with Δr=−18 nm, 0 nm, +18 nm (green, blue, and red curve, respectively). Sharp resonant peaks, corresponding to the excitation of cavity modes, are observed to dominate over an almost flat and weak background emission. In particular, we notice that light-emission at the fundamental cavity mode, occurring at the longest wavelength in the spectra, is strongly enhanced for optimized far-field cavities ($\Delta r = \pm 18$ nm) as compared to the unmodified cavities. This clearly demonstrates the effectiveness of far-field optimization for enhancing the vertical out-coupling efficiency.[15] Besides the fundamental mode, seven additional resonances are clearly visible in the spectra. A comparison with theoretical photonic band structure calculations by means of guided-mode expansion[17] allowed us to identify the whole spectrum of L3 cavity modes in each case, yielding excellent agreement for resonance wavelengths and number of modes (see Fig. 2, top panel).

To understand the origin of the observed sub-bandgap emission from silicon PhC nanocavities, we compared the μPL spectra of an L3 nanocavity with a reference PhC membrane (without cavity), an unpatterned Si-membrane (from SOI), and a reference Czochralski silicon (Cz-Si) sample (Fig. 2). By looking at the spectrum of the bare Si membrane, we can immediately recognize a broad emission band extending from 1.3 to 1.6 μm, which is almost absent in the Cz-Si sample. A similarly broad sub-bandgap emission has previously been reported for bulk c-Si as originating from the rich variety of optically active recombination centers induced by radiation-damage from γ-rays or high-energy ions.[4] Thus, the observation of such a sub-bandgap emission in SOI-based membranes suggests the presence of optically active defects created by the industrial SOI manufacturing process. Indeed, the SmartCut™ technology used by SOITEC is based on high-energy H^+ ion-implantation into a thick Si wafer followed by wafer-bonding and cleaving.[18] Although annealing of the SOI wafer is then performed to remove radiation damage, a small amount of active defects may remain in the thin silicon top layer, giving rise to the observed PL band.

We now consider the effect of PhC patterning on the broad PL emission from the c-Si membrane. An overall increase in light-emission in the whole near-IR range is observed for the patterned PhC membrane as compared to the unpatterned one, which we ascribe to an increased extraction efficiency due to coupling to radiative modes of the Si PhC slab.[19] Notice that emission enhancement is more pronounced for wavelengths below 1.4 μm as compared to the spectral range around 1.5 μm. This is consistent with the strong reduction in electromagnetic density of states in the photonic stop-band (extending from 1.27 to 1.6 μm, see the top panel in Fig. 2). The introduction of additional active recombination centers at the PhC sidewalls by the etching process is also possible. When the far-field optimized L3 nanocavities are considered, a very strong enhancement of the emission is observed as compared to the unpatterned membrane. Focusing our attention only on the fundamental cavity mode around λ=1.55 μm, the enhancement factors can be estimated as $\alpha \simeq 300$, 60, and 250 for Δr=+18 nm, 0 nm, and −18 nm, respectively. Such high values cannot be explained simply by an increased extraction efficiency and represent a clear evidence of Purcell effect acting on the emitting centers coupled to the PhC nanocavity. The Purcell factor F_P can be estimated using simple geometrical considerations on the collection efficiencies η_M and η_C from the bare Si-membrane and the PhC nanocavity, respectively. The collection efficiency for the unpatterned Si-membrane is $\eta_M = 1 - \cos[\sin^{-1}(\mathrm{NA}/n)] = 0.036$, where $n \simeq 3$ is the slab effective refractive index and NA=0.8. Notice that, for NA =1, the collection efficiency coincides with the emission probability into the radiative modes, calculated, e.g., in Ref. 20. On the other hand, an upper limit for the collection efficiencies from our PhC nanocavities is estimated from finite-difference time-domain calculations as $\eta_C = 0.9, 0.2, 0.8$ for Δr=+18 nm, 0 nm, −18 nm, respectively.[15]

Since the maximum increase in extraction efficiency (i.e., without any Purcell effect) is η_C/η_M, the experimental Purcell factor is then given by $F_P \simeq \alpha \eta_M/\eta_C$, yielding very similar values of $F_P \simeq 12$ in each case. This is consistent with the experimental observation that all the three different cavities display almost the same $Q \simeq 3 \times 10^3$ when measured in μPL while independent resonant scattering spectra[21] yield Q-factors of 7.3×10^3, 7.6×10^4, 9.6×10^3 for Δr=+18 nm, 0 nm, −18 nm, respectively, in agreement with theoretical values. To understand this discrepancy, we report in Fig. 3(a) the measured emission intensity and Q factor of the L3 nanocavity with Δr=+18 nm as a function of excitation power. A consistent reduction in the Q-factor is evident as the excitation power is raised from 20 μW up to 1 mW, which we attribute to free-carrier absorption (FCA) induced by the strong pump absorption at λ=532 nm. A similar behavior has been measured for all the cavities. Indeed, a marked blueshift of the nanocavity resonance wavelength is observed for increasing pump powers [Fig. 3(b)], indicating an increase in the mean free-carrier density in the Si slab. This

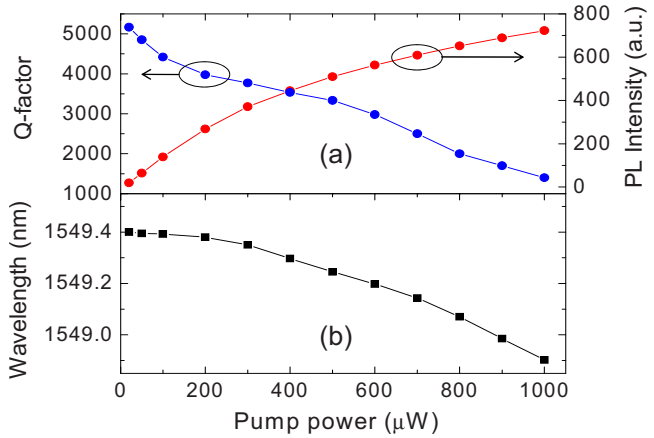

FIG. 3. (Color online) (a) μPL intensity, Q-factor, and (b) resonance wavelength of the L3 cavity with Δr=+18 nm as a function of the excitation power.

demonstrates that Q-factors measured under nonresonant excitation are severely limited by FCA. Higher F_P values are then expected if much lower excitation powers than 500 μW are used in the μPL measurements, though a comparison with the very weak emission from the Si-membrane would become unreliable. Nevertheless, we notice that the above quoted value for F_P is among the highest reported for a PhC nanocavity at room temperature. This result challenges the interpretation of the observed broadband emission as being due to a single (few) inhomogeneously broadened emitter(s), for which a much smaller F_P would occur.[22] Such emission can rather be attributed to a large collection of spectrally distributed narrow-line active centers.

Finally, Fig. 4(a) shows the temperature dependence of light-emission from the modified L3 PhC nanocavity, both on-resonance and off-resonance with the fundamental mode. Surprisingly, the on-resonance μPL is almost constant up to $\simeq$120 K and then slowly decreases for increasing temperatures up to 300 K, where the measured normalized intensity is reduced by a factor 1.6 only. On the other hand, off-resonance PL ($\Delta\lambda$=10 nm) shows a much stronger suppression as a function of temperature, being reduced 10-fold at room temperature. Assuming a simplified model in which the PL thermal quenching, i.e., nonradiative recombination, is governed by two energy levels separated by an activation

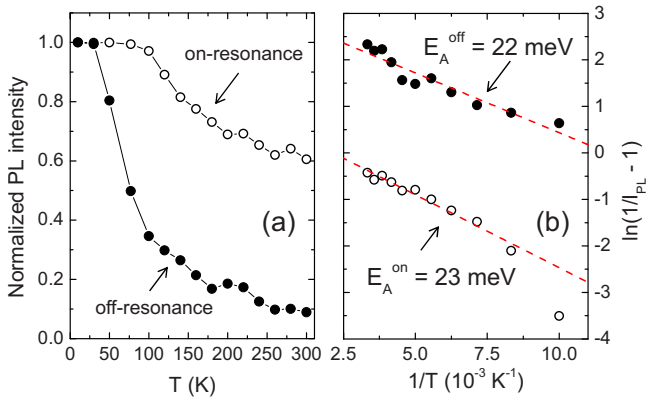

FIG. 4. (Color online) (a) Temperature-dependent PL intensity of the modified L3 nanocavity for on-resonance wavelength (open circles) and off-resonance by $\Delta\lambda\simeq$10 nm (full circles). (b) Arrhenius plots of the high-temperature PL tails for on-resonance (open circles) and off-resonance (full circles) wavelengths. Dashed lines are linear fits to experimental data.

energy E_A (as it is usually assumed for gap-levels in semiconductors), this data may be interpreted through an Arrhenius analysis by plotting the quantity $\ln[1/I_{PL}(T)-1]$ versus $1/T$, as shown in Fig. 4(b). A linear fit of the high temperature tails of the temperature-dependent PL yields very similar activation energies for the on-resonance and the off-resonance PL as $E_A^{on}=23\pm2$ meV and $E_A^{off}=22\pm2$ meV, respectively. Following Ref. 23, since the two activation energies are the same, we can conclude that the persistence of high on-resonance PL values up to room temperature is a further indication of the Purcell effect, leading to an increased internal quantum efficiency due to a larger radiative recombination rate.

In summary, besides providing a useful tool for quick and easy characterization of widespread SOI-based nanostructures, our findings demonstrate the potential of PhC cavities in enhancing even very weak background emission from residual (unintentional) deep-centers in silicon. A much more intense light emission could then be expected by the intentional introduction of a small amount of optically active recombination centers such as dislocation-loops or point-defects in c-Si, opening the route toward the realization of all-silicon light emitting devices at telecom wavelengths.

This work was supported Era-NET NanoSci LECSIN project coordinated by F. Priolo and by the Italian Ministry of University and Research, FIRB Contract No. RBAP06L4S5. The fabrication was carried out in the framework of NanoPiX (see http://www.nanophotonics.eu).

[1]J. M. Shainline and J. M. Xu, Laser Photonics Rev. **1**, 334 (2007).
[2]H. Ennen, G. Pomrenke, A. Axmann, K. Eisele, W. Haydl, and J. Schneider, Appl. Phys. Lett. **46**, 381 (1985).
[3]F. Priolo, G. Franzò, S. Coffa, and A. Carnera, Phys. Rev. B **57**, 4443 (1998).
[4]G. Davies, Phys. Rep. **176**, 83 (1989).
[5]J. Bao, M. Tabbal, T. Kim, S. Charnvanichborikarn, J. Williams, M. J. Aziz, and F. Capasso, Opt. Express **15**, 6727 (2007).
[6]E. Rotem, J. M. Shainline, and J. M. Xu, Appl. Phys. Lett. **91**, 051127 (2007).
[7]E. Ö. Sveinbjörnsson and J. Weber, Appl. Phys. Lett. **69**, 2686 (1996).
[8]S. G. Cloutier, P. A. Kossyrev, and J. M. Xu, Nature Mater. **4**, 887 (2005).
[9]O. Painter, R. K. Lee, A. Scherer, A. Yariv, J. D. O'Brien, P. D. Dapkus, and I. Kim, Science **284**, 1819 (1999).
[10]M. Makarova, V. Sih, J. Warga, R. Li, L. Dal Negro, and J. Vučković, Appl. Phys. Lett. **92**, 161107 (2008).
[11]M. El Kurdi, X. Checoury, S. David, T. P. Ngo, N. Zerounian, P. Boucaud, O. Kermarrec, Y. Campidelli, and D. Bensahel, Opt. Express **16**, 8780 (2008).
[12]S. Iwamoto, Y. Arakawa, and A. Gomyo, Appl. Phys. Lett. **91**, 211104 (2007).
[13]J. S. Xia, Y. Ikegami, K. Nemoto, and Y. Shiraki, Appl. Phys. Lett. **90**, 141102 (2007).
[14]M. Fujita, Y. Tanaka, and S. Noda, IEEE J. Sel. Top. Quantum Electron. **14**, 1090 (2008).
[15]S. L. Portalupi, M. Galli, C. Reardon, T. Krauss, L. O'Faolain, L. C. Andreani, and D. Gerace, Opt. Express **18**, 16064 (2010).
[16]Y. Akahane, T. Asano, B. S. Song, and S. Noda, Nature (London) **425**, 944 (2003).
[17]L. C. Andreani and D. Gerace, Phys. Rev. B **73**, 235114 (2006).
[18]G. Celler and M. Wolf, SOITEC white paper, 2003.
[19]M. Galli, A. Politi, M. Belotti, D. Gerace, M. Liscidini, M. Patrini, L. C. Andreani, M. Miritello, A. Irrera, F. Priolo, and Y. Chen, Appl. Phys. Lett. **88**, 251114 (2006).
[20]C. Creatore and L. C. Andreani, Phys. Rev. A **78**, 063825 (2008).
[21]M. Galli, S. L. Portalupi, M. Belotti, L. C. Andreani, L. O'Faolain, and T. Krauss, Appl. Phys. Lett. **94**, 071101 (2009).
[22]J.-M. Gérard, Top. Appl. Phys. **90**, 269 (2003).
[23]N. Hauke, T. Zabel, K. Muller, M. Kaniber, A. Laucht, D. Bougeard, G. Abstreiter, J. Finley, and Y. Arakawa, New J. Phys. **12**, 053005 (2010).